ARRAYED LIQUID ROTOR ELECTRET POWER GENERATOR SYSTEMS

J. S. Boland, J.D.M. Messenger, H.W. Lo, and Y.C. Tai
California Institute of Technolgy, Pasadena, California, USA

We report our work on liquid rotor electret power generators (LEPG). LEPG devices are essentially fixed-charged, Teflon-electret capacitors with air-filled gaps and liquid droplets that move by vibration. As the liquid moves into and out of the gaps, a net voltage is generated across the capacitor as image charges on the electrodes redistribute according to the position of the droplets. In this work, we also study serial and parallel arrays of LEPG power generators to increase power output. Power output from parallel arrays scales linearly with number of devices, as expected, to produce power output up to about 10 μW. Our initial results show that series arrays need to be studied more because they involve more complicated impedance matching issues.

1. INTRODUCTION

A proliferation of remotely placed sensors, actuators, and electronics is increasingly demonstrating the need for self-sustaining power sources. Specific examples, such as sensor-net nodes and bio-implantable devices, illustrate the difficulties of replacing batteries and the utility of a power source that never needs to be replaced. Energy harvesting, or power scavenging, entails transforming ambient energy into electrical energy. Much work has been dedicated to converting kinetic, light, and heat energy into useable power. The LEPG [1] is the latest energy harvesting device that transforms kinetic energy into electrical energy.

Some successful kinetic energy converters include piezoelectric transducers [2, 3] and electromagnetic generators. Seiko has demonstrated the ability to harvest energy from rotational torque with an electromagnetic power generator in their Kinetic Series watches. We have previously demonstrated this same ability with an electrostatic solution that relies on a permanent electric field produced by an electret [4], which takes advantage of MEMS process efficiencies and produces output voltage swings greater than 40 volts. Our previous generator converts rotational energy to electrical energy with a fixed-charge variable-area capacitor. Exploiting the relationship

$$V(t) = \frac{Q}{C(t)} \tag{1.1}$$

$$C(t) = \frac{\varepsilon A(t)}{d}. \tag{1.2}$$

We are able to convert a variable capacitor area $A(t)$ into a variable voltage for power harvesting. To take advantage of linear oscillations, we could change the geometry of the previous device and fabricate a moving-mass suspended by springs [5]. This is still a fixed-charge, variable-area capacitor. A fixed-charge, variable-distance capacitor is essentially a microphone [6]. The work presented here explores a variable-permittivity capacitor utilizing a liquid dielectric.

$$C(t) = \frac{\varepsilon(t) A}{d} \tag{1.3}$$

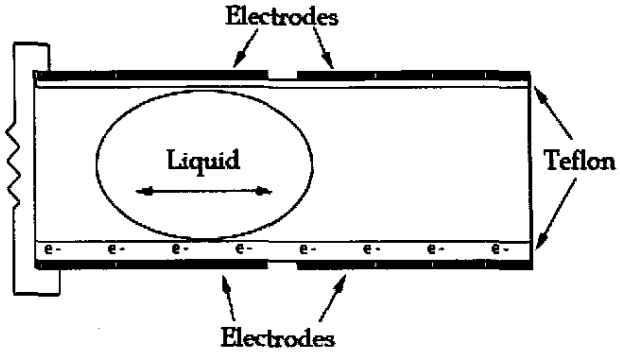

Figure 1. LEPG conceptual image.

The effects of a variable permittivity are explored in freshman E&M books [7], but those examples use a solid dielectric. This would quickly destroy the Teflon surface unless a mechanism is employed to maintain a gap while allowing relative motion. This causes more losses and thus consumes valuable energy. Instead of using solids and more processing steps to create micro springs or sliders, our solution exploits the near-zero friction of a high contact angle liquid on the dielectric.

Experiments with liquid water stalled when the liquid experienced electrowetting [8]. Using silicone oil to prevent electrowetting would enable the use of water, but it is not clear what effect this would have on the required fixed charge. Mercury is a liquid at room temperature, and does not appear to suffer from electrowetting. It has a contact angle of ~150° on Teflon. Mercury, a conductive metal, is equivalent to a dielectric of infinite permittivity.

With negligible friction and heavy mass, the mercury will remain fixed as we subject the capacitor to linear oscillatory motion. Charge that is embedded in Teflon creates a permanent electric field, and the relative motion of mercury to the chamber produces an alternating current at high voltage. The simplicity of this device allows power to be generated without the use of external control circuitry, which would consume power. It is unnecessary to know the liquid's position at any point in time. Furthermore, the driving motion need not be sinusoidal. For the above reasons this new device can be used to harness random, environmental kinetic energy.

0-7803-8732-5/05/$20.00 © 2005 IEEE.

2. THEORY

To model the top and bottom electrodes on the left half of the channel shown in Figure 1., we assume a simple capacitive structure and define

$$C_1(t)=\frac{\varepsilon_{Liquid}\cdot A\cdot x(t)}{G},\quad C_2(t)=\frac{\varepsilon_{teflon}\cdot A\cdot x(t)}{D} \qquad (1.4)$$
$$C_3(t)=\frac{\varepsilon_0\cdot A\cdot(1-x(t))}{G},\quad C_4(t)=\frac{\varepsilon_{teflon}\cdot A\cdot(1-x(t))}{D}$$

corresponding with Figure 2., and use $x(t)$ as a unitless quantity to describe the relative motion of the capacitors to the liquid.

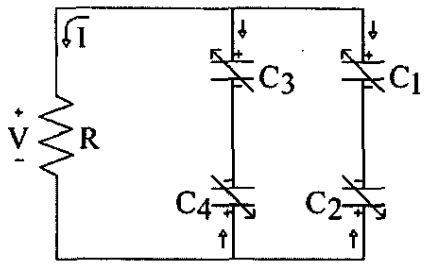

Figure 2. Equivalent circuit for each half of the channel.

Assuming sinusoidal motion of amplitude X_0 and frequency ω, we have

$$x(t)=X_0\cos(\omega t) \qquad (1.5)$$

We use Kirchhoff's Voltage Law

$$V=\frac{Q_1}{C_1}-\frac{Q_2}{C_2}=\frac{Q_3}{C_3}-\frac{Q_4}{C_4} \qquad (1.6)$$

with Q_1, Q_2, Q_3, and Q_4 corresponding to the charge stored on respective capacitors. With implanted charge ρ and capacitor area A, charge conservation give us

$$Q_1+Q_2=\rho\cdot A\cdot x(t),\qquad Q_3+Q_4=\rho\cdot A\cdot(1-x(t)) \qquad (1.7)$$

It follows:

$$Q_2=\frac{-V+\rho Ax(t)\frac{1}{C_1}}{\frac{1}{C_1}+\frac{1}{C_2}} \qquad (1.8)$$

$$Q_4=\frac{-V+\rho A(1-x(t))\frac{1}{C_3}}{\frac{1}{C_3}+\frac{1}{C_4}} \qquad (1.9)$$

By Kirchhoff's Current Law:

$$-\frac{V}{R}+\frac{dQ_2}{dt}+\frac{dQ_4}{dt}=0 \qquad (1.10)$$

We can then take derivatives of (1.8) and (1.9) and substitute them into (1.10). After simplifying, we arrive at an intractable linear first order ODE.

$$V'=\left\{\frac{1}{\frac{C_1C_2}{C_1+C_2}+\frac{C_3C_4}{C_3+C_4}}\right\}\left\{\begin{array}{l}\left\{-\left[\frac{1}{R}+\left(\frac{C_1C_2}{C_1+C_2}+\frac{C_3C_4}{C_3+C_4}\right)'\right]\cdot V\right\}\\ \left\{+\left[\left(\frac{C_2}{C_1+C_2}\right)-\left(\frac{C_4}{C_3+C_4}\right)\right]\cdot\rho Ax'\right\}\end{array}\right. \qquad (1.11)$$

It can be easily verified that equation (1.11) reduces to the well-known RC tank circuit when the capacitors are held constant.

3. FABRICATION

Glass plates are patterned with metal to form capacitor electrodes (Figure 3.). A 25 μm thick film of Teflon FEP is glued to the bottom plate using Teflon AF, which does not provide good adhesion. A 0.5 μm Teflon AF thin film is spun on the top plate to protect the top electrodes from the mercury. The Teflon PTFE layer on the bottom plate is then implanted with electrons from a Welty handheld ion generator to form the electret. The surface voltage was measured to be -850 V before the power generation trials. The spacer (which also defines the liquid chamber) is made by casting Sylgard 184 PDMS onto a CNC-machined mold. Either liquid mercury droplets or a aggregate of steel beads [9] is used to fill half the chamber on the bottom electrode plate. The top electrode plate is then placed on the spacer to finish the device (Figure 3.). Cavity dimensions are W = 1 mm, L = 2 mm, and H = 1 mm with a droplet volume of 1 μL, with 3 columns of 6 cavities per die.

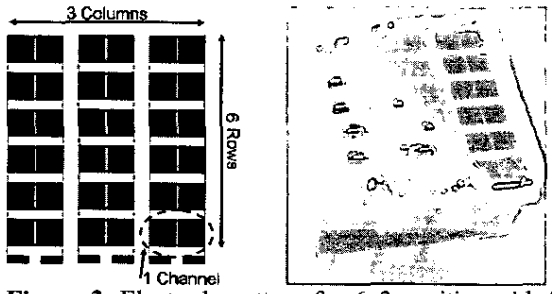

Figure 3. Electrode pattern for 6x3 cavities with 2 top and 2 bottom electrodes per cavity (left) and assembled LEPG device with cutaway (right).

4. EXPERIMENTAL DETAILS

Power generation experiments are performed on a Labworks Inc. ET-139 electrodynamic shaker (Figure 4.) driven sinusoidally by a HP33120A function generator through a Labworks Inc. PA-141 power amplifier. Acceleration is measured using an Endevco 256HX-10 accelerometer. Displacement is acquired by double integration of the acceleration waveform. The shaking frequency can be varied from 20 to 100Hz, and the displacement can be varied from 0 to 5 mm peak-to-peak. The LEPG's output voltage across a load resistor is measured with a National Semiconductor LF356N op-amp used as a 10^{12} Ohm impedance voltage buffer. Both acceleration and generator voltage waveforms are averaged over 256 samples on an HP oscilloscope and captured to computer by IntuiLink software over GPIB.

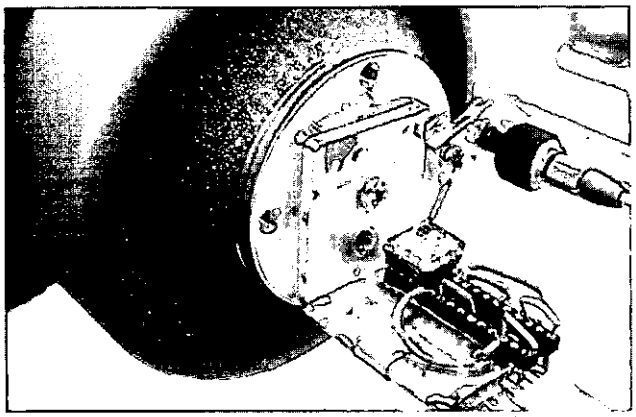

Figure 4. Test setup for LEPG mounted on shaker

5. DATA

With the top electrodes replaced by a glass slide, using high-speed video we can clearly see the motion of the channels and the mercury droplets within. Shaking at low amplitudes and above 20Hz with the channels perpendicular to gravity, the mercury droplets remain fixed in space while the channels move about them. By increasing the amplitude to at least half the channel length, we see that the droplets' centers of mass are well synchronized but no longer stationary. Impacts with the ends of the cavities impart energy to the mercury droplets that is converted into deformation of the surface (as shown in Figure 5b.). When the walls and the droplets have zero relative velocity, the energy of surface deformation is transferred back into kinetic energy of the droplets. This process increases the relative motion of the droplets, and is reflected in the output waveforms as phase lag (Figure 8.) and larger currents with reduced duty cycle. The increase in power output in this overdriving mode is smaller than the increase in input energy. While overdriving the amplitude ensures synchronization, it is rarely the case that the channels are perfectly perpendicular to gravity, and overdriving may be unnecessary. Replacing the mercury with aggregates of steel beads demonstrates no phase lag and also benefits from overdriving [9].

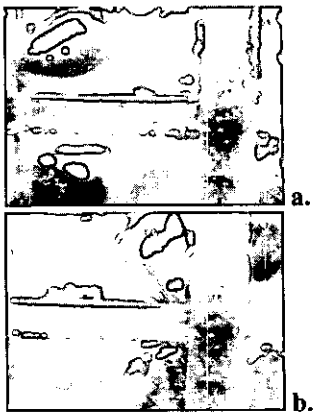

Figure 5. Still-frames taken at 2000fps while shaking at 60Hz and 1 mm peak to peak amplitude.

Parallel Arrays

By design, the arrayed devices are organized in 3 columns, where every column contains 6 devices in parallel (Figures 1. and 2.). Each device in the array contains an electrode pair on each half of the channel. For the purposes of this test, only the electrodes on the left side of the channels are tested. We take data from 1, 2, or 3 columns in parallel (Figure 6.). Data shows power output scaling linearly with number of devices in parallel. Testing smaller arrays with 4 and 5 devices per column produced similar results.

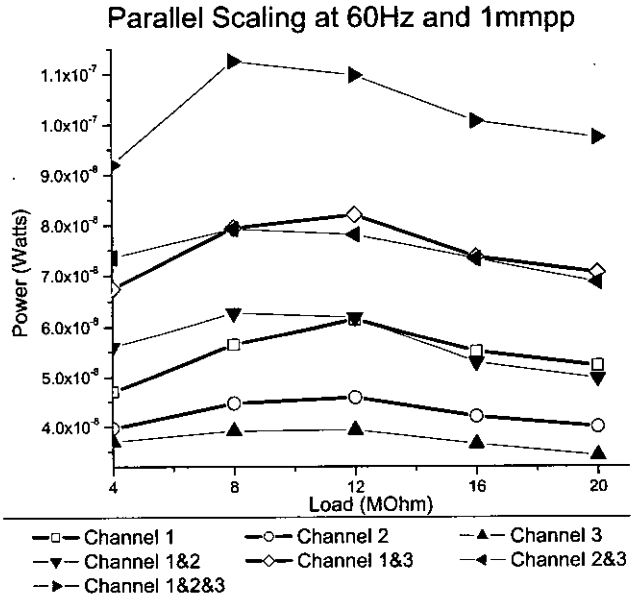

Figure 6. Experimental values for parallel channels shaking of 2.58 mm peak-to-peak at 60Hz. Theoretical values for parallel channels shaking of 1 mm p-p.

Serial Arrays

After tests demonstrated the linear scaling of parallel arrays, we used the same columns of 6 electrodes, but this time the electrodes between the columns were connected serially. The relationship is anything but linear in this case, and any columns in serial produce less power output than single columns. The waveforms are shown in Figure 6., which shows voltage vs. time for each column and combinations of those columns. These results imply complicated interactions between columns, probably related to slight phase differences and feedback effects. Testing with 4 and 5 electrode columns produced similar results.

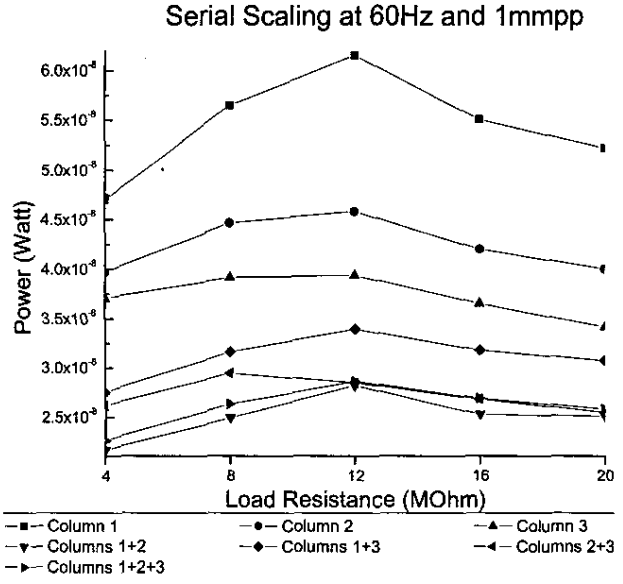

Figure 7. Experimental values for serial columns shaking at 1 mm peak-to-peak at 60Hz.

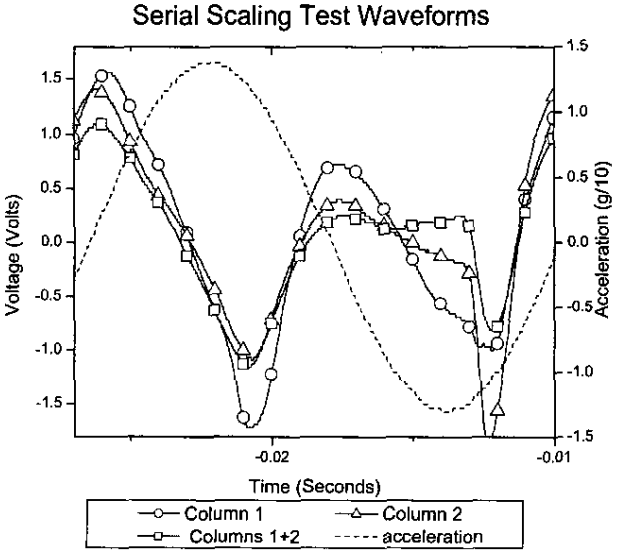

Figure 8. Experimental values for shaking at 2.58 mm peak-to-peak at 60 Hz and load resistance of 4 MOhm.

6. CONCLUSIONS

This work demonstrated the ability to connect many LEPG devices in parallel, and the difficulty with serially connected LEPG devices. Devices in parallel allow for increased power output, and also allow for the possibility of creating further miniaturized and embedded power systems. Future work will concentrate on better load matching of LEPG and smaller channels.

This work is supported by DARPA MPG program (DAAH01-01-1-R002) and NSF ERC Center for Neuromorphic Systems Engineering at Caltech (EEC-9402726).

7. REFERENCES

[1] J. S. Boland and Y.-C. Tai, "Liquid-Rotor Electret Micropower Generator," presented at Solid-State Sensor, Actuator, and Microsystems Workshop, Hilton Head Island, South Carolina, 2004.

[2] N. Shenck and J. Paradiso, "Energy scavenging with shoe-mounted piezoelectrics," in *IEEE Micro*, vol. 21, 2001, pp. 30-42.

[3] S. Roundy, P. K. Wright, and J. Rabaey, "A study of low level vibrations as a power source for wireless sensor nodes," *Computer Communications*, vol. 26, pp. 1131-1144, 2003.

[4] J. Boland, Y.-H. Chao, Y. Suzuki, and Y. C. Tai, "Micro Electret Power Generator," presented at IEEE The Sixteenth Annual International Conference on Micro Electro Mechanical Systems, Kyoto, Japan, 2003.

[5] Y. Suzuki and Y. C. Tai, "Micromachined high-aspect-ratio parylene beam and its application to low-frequency seismometer," presented at IEEE The Sixteenth Annual International Conference on Micro Electro Mechanical Systems, Kyoto, Japan, 2003.

[6] W. Hsieh, T. Hsu, and Y. Tai, "A Micromachined Thin-Film Teflon Electret Microphone," presented at TRANSDUCERS '97, Solid-State Sensors and Actuators, Chicago; IL, 1997 Jun.

[7] D. J. Griffiths, *Introduction to Electrodynamics*, Second ed. Upper Saddle River: Prentice Hall, 1989.

[8] H. Moon, S. Cho, R. Garrell, and C. Kim, "Low-voltage electrowetting-on-dielectric," *Journal of applied physics*, vol. 92, pp. 4080-4087, 2002.

[9] J. S. Boland, J. D. M. Messenger, and Y.-C. Tai, "Alternative Designs of Liquid Rotor Electret Power Generator Systems," presented at The Fourth International Workshop on Micro and Nanotechnology for Power Generation and Energy Conversion Applications, Kyoto, Japan, 2004.